Proceedings of the Canadian Society for Mechanical Engineering International Congress 2022
CSME Congress 2022
June 5-8, 2022, Edmonton, AB, Canada

Free Convection Heat Transfer of Nano-enhanced Phase Change Material in a Porous Medium

Sahar Goudarzi[1], Xili Duan[1], Greg F. Naterer[1], Yuri Muzychka[1]
[1]Department of Mechanical Engineering, Memorial University of Newfoundland St. John's, NL, Canada A1B 3X5

Abstract. This paper aims to evaluate the effect of porosity and buoyancy on the natural convection of CuO-RT25 nano-enhanced phase change material (NePCM) in a differentially heated porous square cavity. Buongiorno's two-phase model is utilized to consider the Brownian thermophoresis diffusion of nanoparticles in the carrier liquid. The governing equations are solved numerically by a finite volume technique. The numerical solution is performed using the Brinkman–Forchheimer-extended Darcy model and Boussinesq approximations, as well as the non-equilibrium thermal boundary condition for the porous media. Numerical computations are performed for various Rayleigh numbers ($Ra=5\times10^3$, $Ra=3\times10^5$) and porosity ratios ($\varepsilon=0.7, 1$). Effects of porosity, buoyancy, and nanoparticle distribution on the flow and heat transfer rates are discussed in detail by isotherms and distributions of nanoparticles. Numerical results indicate that at $Ra=3\times10^5$, heat is transferred via conduction at the beginning and its rate is not significantly affected by porosity. As time passes, the convection mechanism increasingly affects the temperature profiles, while conduction remains the dominant heat transfer mechanism in the porous media at a lower Rayleigh number.

Keywords: Nano-enhanced PCM, Energy Storage, Porous medium, Buongiorno's model

I. INTRODUCTION

Thermal energy storage (TES) enables systems to balance the demand and supply needs of renewable energy sources [1 - 2]. PCM (phase change material) is a material that can absorb and release thermal energy by melting and freezing/cooling. It undergoes phase change at its fusion temperature. PCMs are effective in enhancing the energy efficiency. PCMs are known for their low thermal conductivity, which restricts their use in industry. Some methods to address this shortcoming include nanofluid addition and porous media. Nanofluids can be introduced to enhance the thermophysical properties of the working fluid [3 - 5]. A porous medium is a solid structure or matrix containing voids or pores through which one or more fluids can pass. The porous structure is between a micropore to macropore size (>0.6 nm and <200 mm). The porous structure affects thermostabilizing and the phase change behaviour of PCMs in the smaller-scale pores [6].

In nanofluid processes, two main approaches are commonly taken; single-phase and two-phase modelling. The first approach considers the combination of nanoparticles and base fluid as a homogenous (single-phase) mixture with uniform properties. Also, thermal equilibrium is considered between the nanoparticles and the base fluid. In contrast with the single-phase approach, two-phase modelling introduces nanoparticle properties and behaviours separately from the base fluid properties and behaviours [7].

From results of Abdoljamal and Vafaei [8], the single-phase model shows good agreement with experimental studies. But the discrete phase model overestimates the heat transfer coefficient, while the mixture model may show unrealistic results compared to experimental results. Some experimental studies have questioned the validity of a single-phase model [9]. Considering a slip velocity between nanoparticles and base fluid is the most common approach to simulate nanofluids in a two-phase model. Buongiorno [10] considered seven slip mechanisms. The study showed that Brownian diffusion and thermophoresis effects are crucial slip mechanisms for nanofluids from these seven slip mechanisms. The experimental studies have demonstrated that a two-phase approach better predicts the nanofluids [11].

Moreno et al. [12] studied the heat transfer inside a cubic cavity filled with air. They considered a vertical wall with phase change material experimentally and numerically to determine thermal energy storage features. According to their results, the uneven temperature gradient at the wall is due to the buoyancy effect, while PCMs augment the heat transfer. The mixture of PCMs and ultra-small nanomaterials are called nano-enhanced phase change material (Nano-PCMs). Thermophysical properties of the base PCM such as the latent heat of fusion, viscosity, super-cooling degree, specific heat, density, and phase change temperature can change by dispersing nanoparticles [13].

Dhaidan et al. [14] studied the melting of nano-enhanced PCM (octadecane-CuO) numerically and experimentally. Based on their studies, not only an enhancement in thermal conductivity of the PCM is seen by adding the nanoparticles but also an improvement in melting characteristics is noticed. For instance, the melting rate increases, and the charging time accelerates. As the Rayleigh number increases, an earlier onset of natural convection happens, which accelerates the melting process.

Three cases have been investigated by Al-Kayiem and Owolabi [15], including a case without PCM, with PCM and with Nano-enhanced PCM (NePCM) to illustrate the effects of

PCM and NePCM in solar collector performance. According to their results, the solar collector has the best performance by adding the NePCM. Its performance improved by 8.4% by using NePCM, while it was enhanced 6.9% by using the PCM.

Li et al. [16] investigated a porous medium and nanoparticle effects on the thermal conductivity of PCM. They studied four cases, including PCM, NePCM, porous-PCM, and porous-NePCM. They reported that the melting and solidification time decreases by 25.9% and 28.2%, respectively, as the nanoparticle concentration rises with an 83.7% and 88.2% time reduction in melting and solidification, respectively. Moreover, for the porous-NePCM situation, melting and solidification time decreases to 84.2% and 88.8% respectively.

Hu and Gong [17] studied the thermal performance of the phase change material in the porous medium. They reported the melting time decreases by about 38% by embedding PCM in the porous medium and concluded that saturation of porous metal structure into the porous metal could improve the thermal efficiency of the PCM.

This paper further examines nano-enhanced phase change materials as an innovative approach in energy storage that can overcome the low thermal conductivity limitations of PCMs. The porous medium is demonstrated as an approach to augment the heat transfer rates.

II. Problem Definition

Natural convection of Nano-enhanced Phase change material is studied in this paper. The slip velocity is taken into account as nanoparticles are dispersed in the porous medium. The porous medium is a cavity with a height L. Fig.1 shows a schematic of the defined problem in which the NePCM is dispersed in a porous medium. The right and left walls are cold and hot, respectively, while the top and bottom walls are adiabatic. Natural convection of Nano-enhanced phase change material occurred due to density variations and buoyancy.

III. Formulation and Numerical Method

In this study, the Buongiorno two-phase model is extended to incorporate Brownian, thermophoresis dispersion of nano-enhanced phase change materials inside a porous enclosure. It is assumed that the base fluid is incompressible, no chemical reactions occurs between the particles, the average volume fraction is less than 0.06, viscous dissipation is negligible, radiative heat transfer is negligible, and thermal equilibrium exists between nanoparticles.

The liquid PCM is considered an isotropic and incompressible Newtonian fluid. The porous medium is considered an open-cell, homogeneous and isotropic. In the thermal non-equilibrium model, the porous medium and fluid are not in thermal equilibrium and the temperatures of the solid and the fluid are solved separately using a semi-heuristic approach based on a local thermal non-equilibrium model.

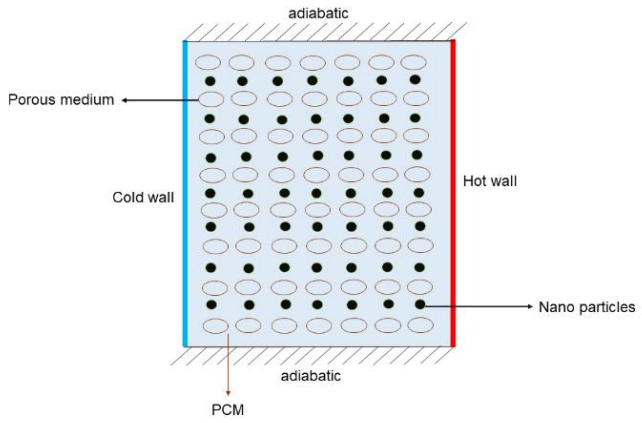

Fig.1 Schematic of the problem.

Open FOAM software is used to solve the Navier-Stokes equations. A FVM method and PIMPLE algorithm is used. The PIMPLE Algorithm is a combination of PISO-Pressure Implicit with Splitting of Operator- and SIMPLE -Semi-Implicit Method for Pressure-Linked Equations. It is applied to couple the pressure and velocity considering the Boussinesq approximation. First-order schemes of Bounded Gauss upwind methods are utilized for the divergence of the velocity and temperature. Moreover, for solving the gradient terms, a second-order least squares scheme is used. When solving the Laplacian terms, the Gauss linear orthogonal method is used. Residuals for the velocity and pressure are calculated to be less than 10^{-6}, while it is less than 10^{-8} for the temperature.

Based on these assumptions, the governing equations for the Brinkman–Forchheimer-extended Darcy model are given as follows [18]. For the continuity equation

$$\varepsilon \partial \rho_{nf} / \partial t + \nabla . \rho_{nf} \vec{V} = 0 \tag{1}$$

where nf represents nanofluid properties. For the momentum equation in the x direction [20]:

$$\frac{\rho_{nf}}{\varepsilon}\frac{\partial u}{\partial t} + \frac{\rho_{nf}}{\varepsilon^2}\left(\vec{V}.\nabla u\right) = -\frac{\partial P}{\partial x} + \left(\frac{\mu_{nf}}{\varepsilon}\nabla u^2\right) - \frac{A_m(1-\lambda)^2}{\lambda^3+0.001}u - \left(\frac{\mu_{nf}}{K} + \frac{\mu_{nf}C|u|}{\sqrt{K}}\right)u \tag{2-a}$$

The momentum equation in the y direction [19] is given by:

$$\frac{\rho_{nf}}{\varepsilon}\frac{\partial v}{\partial t} + \frac{\rho_{nf}}{\varepsilon^2}\left(\vec{V}.\nabla v\right) = -\frac{\partial P}{\partial y} + \left(\frac{\mu_{nf}}{\varepsilon}\nabla v^2\right) - \frac{A_m(1-\lambda)^2}{\lambda^3+0.001}v - \left(\frac{\mu_{nf}}{K} + \frac{\mu_{nf}C|v|}{\sqrt{K}}\right)v + (\rho\beta)_{nf}\varepsilon\cdot(T-T_{Ref})g \tag{2-b}$$

The second term of the right side of the momentum equation belongs to viscous resistance and the third term is the Kozeny-Carman term in which $A_m = \frac{10^5 kg}{m^3 s}$ [20]. The fourth and fifth terms represent the extension of Darcy's law to explain the non-Darcy effects. The sixth term in the y-direction accounts for the gravitational effects due to the Boussinesq approximation. The first term related to the presence of the porous medium is the viscous loss term [21] where

$$K=0.00073\, d_p^{2}(1-\varepsilon)^{-0.224}\left(\frac{d_l}{d_p}\right)^{-1.11}$$

This is calculated based on experimental results [21]The inertial loss term C is determined as

$$C=0.00212(1-\varepsilon)^{-0.132}\left(\frac{d_l}{d_p}\right)^{-1.63}$$

Here d_l is the ligament or cell diameter and d_p is the pore size and defined as

$$d_l=1.18dp\sqrt{\frac{1-\varepsilon}{3\pi}}\left(\frac{1}{1-e^{-(1-\varepsilon)/0.04}}\right)$$

$$d_p=0.0254(m)/\omega\ (PPI)$$

PPI refers to pores per inch [22].

The energy equation for NePCM and the porous medium are given as (NePCM):

$$\varepsilon\rho_l\left(Cp_m+L\frac{d\lambda}{dT_l}\right)\frac{\partial T_l}{\partial t}+\rho_l Cp_m(V.\nabla T)=(k_{fe}\ \nabla^2 T_l)-h_{sf}A_{sf}(T_l-T_s)-(Cp)_m J_{np}.\nabla T \quad (3)$$

where np,fe,m,l, and s subscripts stand for nanoparticle, effective fluid thermal conductivity, mixture, liquid, and solid.

For a porous medium:

$$(1-\varepsilon)\rho_{pr}Cp_{pr}\frac{\partial T_s}{\partial t}=(k_{se}\ \nabla^2 T_l)-h_{sf}A_{sf}(T_l-T_s) \quad (4)$$

where pr, s, and se subscripts represent the porous medium, solid, and effective solid thermal conductivity, respectively. Also, h_{sf} is the local heat transfer coefficient while A_{sf} is the specific surface area.

Moreover, in these equations λ is given by:

$$\lambda=\frac{\Delta H}{L}=\begin{cases}0 & \text{if } T<T_S\\ 1 & \text{if } T>T_L\\ \dfrac{T-Ts}{T_l-Ts} & \text{if } T_S<T<T_L\end{cases}$$

Total enthalpy is given by:

$$H=h+\Delta H \quad (5)$$

In which h is:

$$h=h_{ref}+\int_{T_{ref}}^{T}CpdT \quad (6)$$

Here h_{ref} is the sensible enthalpy at the reference temperature and T_{ref} is the reference temperature. In the thermal non-equilibrium model, the effective thermal conductivity of the fluid and solid should be determined and employed independently

.

In this simulation the Boomsma and Poulikakos model [23] is employed:

$$k_m=\frac{k_{np}+2k_l-2\varphi(k_{np}-k_l)}{k_{np}+2k_l+\varphi(k_{np}-k_l)} \quad (7)$$

$$k_{eff}=\frac{1}{\sqrt{2}(R_A+R_B+R_C+R_D)_{4\sigma}} \quad (8)$$

$$R_A=\frac{}{(2e^2+\pi\sigma(1-e))k_s+(4-2e^2-\pi\sigma(1-e))k_m} \quad (9)$$

$$R_B=\frac{(e-2\sigma)^2}{(e-2\sigma)e^2k_s+(2e-4\sigma-(e-2\sigma)e^2)k_m} \quad (10)$$

$$R_C=\frac{\sqrt{2}-2e}{\sqrt{2}\pi\sigma^2k_s+(2-\sqrt{2}\pi\sigma^2)k_m} \quad (11)$$

$$R_D=\frac{2e}{e^2k_s+(4-e^2)k_m} \quad (12)$$

where e=0.16 and $\sigma=\sqrt{\frac{\sqrt{2}(2-\frac{3\sqrt{2}}{4}e^3-2\varepsilon)}{(3-2\sqrt{2}e-e)\pi}}$. Also, $k_{fe}=k_{eff}|k_{se}=0$ and $k_{se}=k_{eff}|k_{fe}=0$

Nano particle dispersion equations are given as follows [10]:

$$\frac{1}{\varepsilon}\vec{V}.\nabla\varphi=-\frac{1}{\rho_{np}}\nabla.(\overrightarrow{J_{np}}) \quad (13)$$

$$\overrightarrow{J_p}=\overrightarrow{J_B}+\overrightarrow{J_T} \quad (14)$$

$$\overrightarrow{J_B}=-\rho_{np}D_B\nabla\varphi, \quad (15)$$

$$\overrightarrow{J_T}=-\rho_{np}D_T\frac{\nabla T}{T} \quad (16)$$

$k_B=1.380648\times10^{-23}$ J/K

where

$$D_B=\frac{k_BT}{3\pi\mu_f d_{np}},\ D_T=\gamma\frac{\mu_{pcm}}{\rho_{pcm}}\varphi \text{ and } \gamma=0.26\frac{k_{pcm}}{k_{pcm}+k_{np}}$$

The equations for nanoparticle distribution include the Brownian motion, and thermophoresis motion, where B and T subscripts represent these motions respectively.

Properties of the mixture can be determined as [24]:

$$\rho_m=(1-\varphi)\rho_{pcm}+\varphi\rho_{np} \quad (17)$$

$$\mu_m=\frac{\mu_{pcm}}{(1-\varphi)^{2.5}} \quad (18)$$

$$\beta_m=\frac{(1-\varphi)\rho_{pcm}\beta_{pcm}+\varphi\rho_{np}\beta_{np}}{\rho_m} \quad (19)$$

Furthermore, PCM properties are listed below [25]:

$$\gamma=0.5\text{erf}(4\frac{(T-T_m)}{T_l-T_s})+0.5 \quad (20)$$

$$\rho_{pcm}=(1-\gamma)\rho_s+\gamma\rho_l \quad (21)$$

$$k_{pcm}=(1-\gamma)k_s+\gamma\rho_l \quad (22)$$

$$\beta_{pcm}=\frac{(1-\gamma)\rho_s\beta_s+\gamma\rho_l\beta_l}{\rho_{pcm}} \quad (23)$$

Table 1: Thermophysical properties of porous medium and CuO

	$\rho(\frac{kg}{m^3})$	$k(\frac{W}{mK})$	$Cp(\frac{J}{kgK})$	$\beta\times10^{-5}(\frac{1}{K})$	$d_p(nm)$
porous	1978.6	1.1293	-	–	0.05
CuO	6500	18	540	0.85	30

Thermophysical properties of the porous medium nanoparticle and PCM are presented in Tables 1 and 2 respectively.

Table 2: Thermophysical properties of RT25

RT25	Value
Density, solid phase	880 kg/m3
Density, liquid phase	760 kg/m3
Dynamic viscosity, liquid phase	0.02 Pa s
Specific heat (both phases)	2000 J/kgK
Thermal conductivity (both phases)	0.2 W/mK
Latent heat	189 kJ/kg
Solidus temperature	24.5 °C
Liquidus temperature	26.5 °C

IV. RESULTS AND DISCUSSION

Grid independence is analyzed for important parameters such as the Nusselt number at the wall. As illustrated in Fig 2, the 20,000 node mesh is appropriate for grid independent simulations.

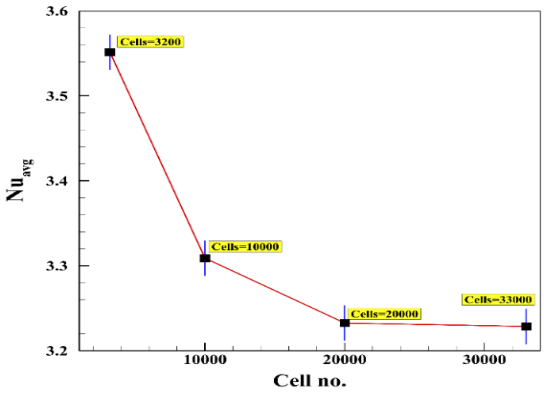

Fig.2 Mesh convergence study based on Nusselt number variation

Table 3 compares two-phase nanoparticle dispersion of the current study with an experimental study of Ho et al [27] where it is clarified this study is in good agreement with the experimental study.

Table.3 Nusselt number comparison of the current study with Ho et al.[26]

	$Ra = 6.7\times10^5$	$Ra = 10\times10^5$	$Ra = 13\times10^5$
Ho et al.[26]	$Nu = 7.2769$	$Nu = 9.1765$	$Nu = 9.7230$
Current	$Nu = 7.8234$	$Nu = 9.0078$	$Nu = 9.4277$

Fig. 3 presents a comparison of the phase change material inside a cavity with the current study and an experimental study of melting behavior of phase change material in an enclosure at various times. Moreover, Fig. 4 compares interface points of the current study with experimental results. As illustrated, the simulation is in a good agreement with experimental results carried out by Kamkari et al [27].

The current study investigates the effects of buoyancy forces (Rayleigh number), porosity, and nanoparticle volume fraction on natural convection. Brownian diffusion and thermophoresis effect are taken into account in the nanofluid simulation. For this simulation $5\times10^3 \le Ra \le 3\times10^5$, $0.7\le\varepsilon\le1$ and $0\le\varphi\le0.04$. Figure 5 illustrates isothermal lines of NePCM fluid flow at $Ra=3\times10^5$. This illustration compares the isothermal lines inside a porous medium ($\varepsilon=0.7$) and non-porous ($\varepsilon=1$) medium. *A* lower temperature gradient happens in the presence of a porous medium during the melting process.

For the non-porous case at $Ra=3\times10^5$, the buoyancy force is dominant in the flow; as a result, isothermal lines circulate faster in comparison with the porous case. On the other hand, when porosity comes into account, the conduction term mainly affects the flow at the beginning; as time passes, the convection mechanism becomes dominant.

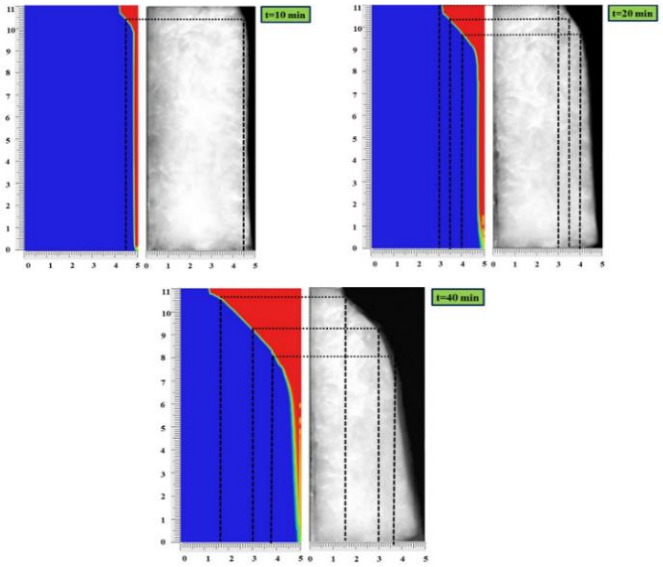

Fig.3 Comparison with experimental results of Kamkari et al [27]

Due to the higher flow resistance in a porous medium, convection has a subtle effect on temperature gradient compared to the non-porous case. Moreover, as demonstrated in a porous medium, heat is transferred more uniformly between layers compared to the NePCM case only. Figure 5 demonstrates the same process for lower Rayleigh numbers $Ra=5\times10^3$. As can be seen, isothermal lines are nearly parallel at the beginning in both cases, indicating that conduction is the dominant mechanism in heat transport. After some time, the convection heat transfer in non-porous cases affects the isothermal lines, and as illustrated, low thermal conductivity of the PCM circulates due to the natural convection. Moreover, for the porous cases, as time passes, the conduction heat transfer stays as a dominant heat transfer mechanism; as a result, the isothermal lines remain parallel.

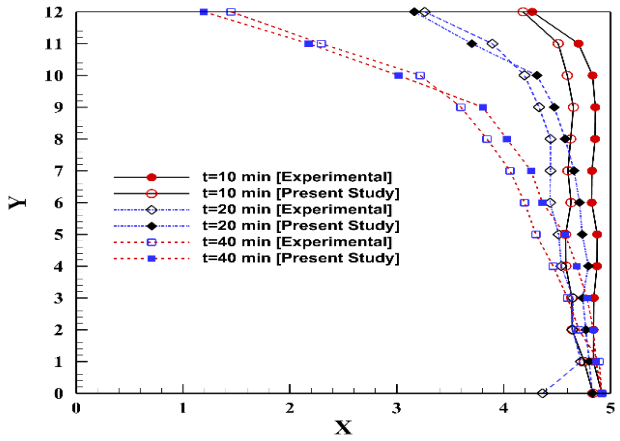

Fig.4 Comparison with experimental study of interface points

Figures 6 and 7 demonstrate nanoparticle dispersion due to Brownian motion and thermophoresis diffusion. The left wall is the hot wall while the right wall is the cold wall. For all cases, nanoparticle dispersion near the cold wall is more pronounced than the dispersion near the hot wall. This phenomenon occurs due to thermophoresis diffusion. As porosity increases, the maximum nanoparticle dispersion decreases as the Brownian motion of nanoparticles is lower when increasing the porosity.

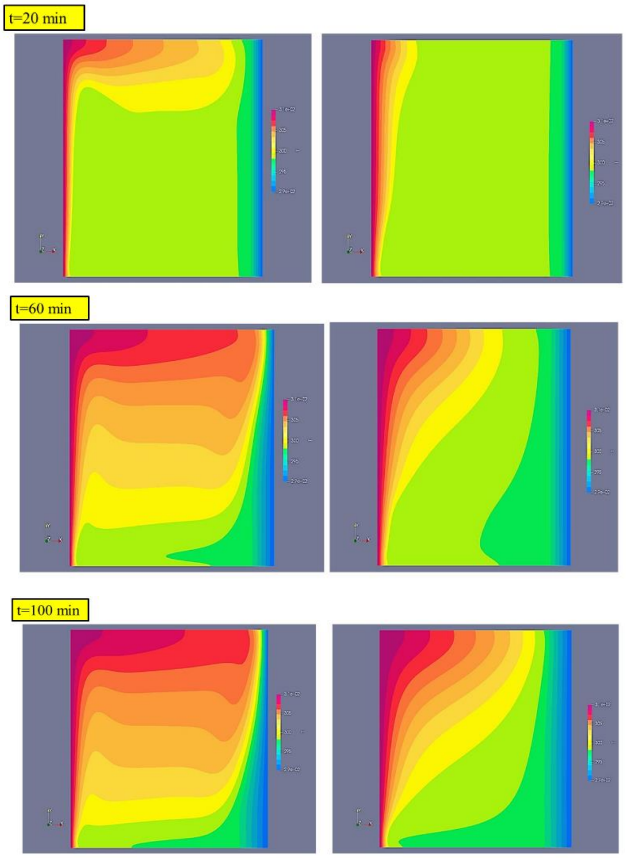

Fig.5 Isothermal lines at Ra=3×10^5 where left side stands for non-porous medium while the right side is in a porous medium with ε=0.7

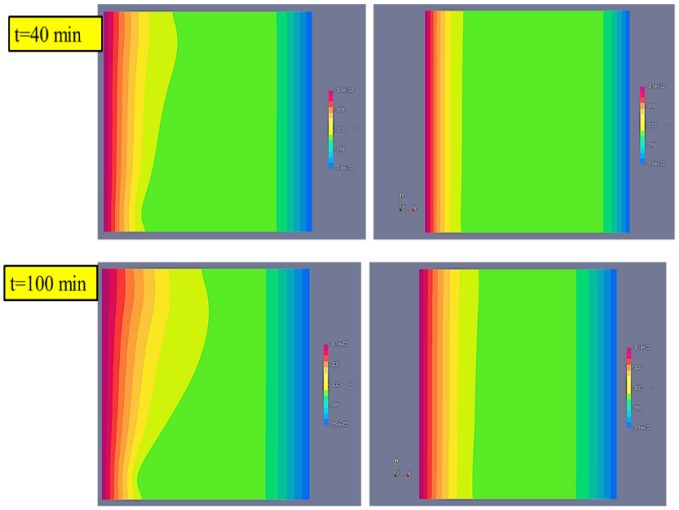

Fig.6 Isothermal lines at Ra=5×10^3 where left side stands for non-porous medium while the right side is in a porous medium with ε=0.7

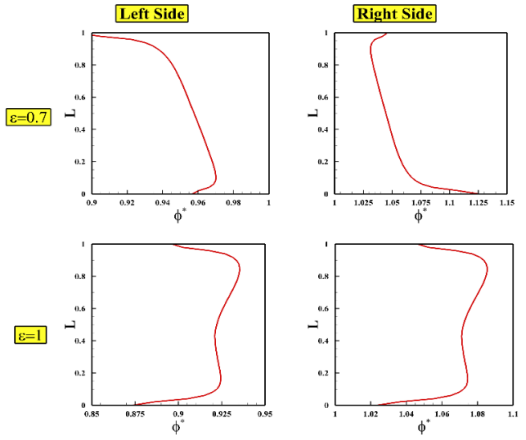

Fig.7 Nanoparticle distribution on right and left walls at Ra=5×10^3

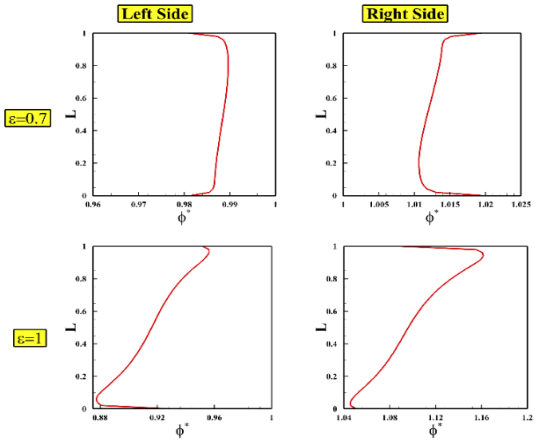

Fig.8 Nanoparticle distribution on right and left walls at Ra=3×10^5

V. CONCLUSIONS

The impacts of buoyancy forces and porosity on the natural convection of a nano-enhanced phase change material inside an

enclosure is studied by the finite volume method and a two-phase model. The effects of some critical parameters such as Rayleigh number, porosity ratio of the porous media, temperature, and nanoparticle distribution are presented. It has been shown that thermophoresis effects lead to the migration of particles from the hot to cold wall. Also, for a given value of Rayleigh number, the nanoparticle volume fraction decreases along the sidewalls by increasing the porosity, due to the reduction in Brownian motion. A decrease is observed in temperature gradient in the presence of the porous medium. For all cases, initially, the conduction term mainly affects the flow, but as time passes, the convection mechanism becomes activated.

VI. ACKNOWLEDGEMENTS

The authors gratefully acknowledge the financial support of this research from the Natural Sciences and Engineering Research Council of Canada (NSERC).

REFERENCES

[1]. Guo, Hao, Kun Qian, Anjiang Cai, Jun Tang, and Jun Liu. "Ordered gold nanoparticle arrays on the tip of silver wrinkled structures for single molecule detection." *Sensors and Actuators B: Chemical* 300 (2019): 126846.

[2]. Newell, Richard, Daniel Raimi, and Gloria Aldana. "Global energy outlook 2019: the next generation of energy." *Resources for the Future* 1 (2019): 8-19.

[3]. Tawfik, Mohamed M. "Experimental studies of nanofluid thermal conductivity enhancement and applications: A review." *Renewable and Sustainable Energy Reviews* 75 (2017): 1239-1253.

[4]. Mohamed, Mousa M., Nabil H. Mahmoud, and Mohamed A. Farahat. "Energy storage system with flat plate solar collector and water-ZnO nanofluid." *Solar Energy* 202 (2020): 25-31.

[5]. Pandya, Naimish S., Harshang Shah, Maysam Molana, and Arun Kumar Tiwari. "Heat transfer enhancement with nanofluids in plate heat exchangers: A comprehensive review." *European Journal of Mechanics-B/Fluids* 81 (2020): 173-190.

[6]. Vafai, Kambiz, ed. *Handbook of porous media*. Crc Press, 2015.

[7]. Saghir, M. Ziad, A. Ahadi, Tooraj Yousefi, B. Farahbakhsh. "Two-phase and single phase models of flow of nanofluid in a square cavity: comparison with experimental results." *International Journal of Thermal Sciences* 100 (2016): 372-380.

[8]. Albojamal, Ahmed, and Kambiz Vafai. "Analysis of single phase, discrete and mixture models, in predicting nanofluid transport." *International Journal of Heat and Mass Transfer* 114 (2017): 225-237.

[9]. Ying, Zhaoping, Boshu He, Di He, Yucheng Kuang, Jie Ren, and Bo Song. "Comparisons of single-phase and two-phase models for numerical predictions of Al2O3/water nanofluids convective heat transfer." *Advanced Powder Technology* 31 (2020): 3050-3061.

[10]. Buongiorno, Jacopo. "Convective transport in nanofluids." (2006): 240-250.

[11]. Wen, Dongsheng, and Yulong Ding. "Experimental investigation into convective heat transfer of nanofluids at the entrance region under laminar flow conditions." *International journal of heat and mass transfer* 47, no. 24 (2004): 5181-5188.

[12]. Moreno, S., J. F. Hinojosa, I. Hernández-López, and J. Xaman. "Numerical and experimental study of heat transfer in a cubic cavity with a PCM in a vertical heated wall." *Applied Thermal Engineering* 178 (2020): 115647.

[13]. Yang, Xun, Teng Xiong, Jing Liang Dong, Wen Xin Li, and Yong Wang. "Investigation of the dynamic melting process in a thermal energy storage unit using a helical coil heat exchanger." *Energies* 10, no. 8 (2017): 1129.

[14]. Dhaidan, Nabeel S., J. M. Khodadadi, Tahseen A. Al-Hattab, and Saad M. Al-Mashat. "Experimental and numerical investigation of melting of NePCM inside an annular container under a constant heat flux including the effect of eccentricity." *International Journal of Heat and Mass Transfer* 67 (2013): 455-468.

[15]. Saw, C. L., Hussain H. Al-Kayiem, and Afolabi L. Owolabi. "Experimental investigation on the effect of PCM and nano-enhanced PCM of integrated solar collector performance." *WIT Transactions on Ecology and Environment* 179 (2013): 899-909.

[16]. Li, Z., A. Shahsavar, A. Al-Rashed, and Pouyan Talebizadehsardari. "Effect of porous medium and nanoparticles presences in a counter-current triple-tube composite porous/nano-PCM system." *Applied Thermal Engineering* 167 (2020): 114777.

[17]. Hu, Xusheng, and Xiaolu Gong. "Experimental and numerical investigation on thermal performance enhancement of phase change material embedding porous metal structure with cubic cell." *Applied Thermal Engineering* 175 (2020): 115337.

[18]. Zhang, P., X. Xiao, Z. Meng, M. Li. "Heat transfer characteristics of a molten-salt thermal energy storage unit with and without heat transfer enhancement." *Applied Energy* 137 (2015): 758-772.

[19]. Nield, Donald A., and Adrian Bejan. *Convection in porous media*. Vol. 3. New York: springer, 2006.

[20]. Xu, Yang, Qinlong Ren, Zhang-Jing Zheng, and Ya-Ling He. "Evaluation and optimization of melting performance for a latent heat thermal energy storage unit partially filled with porous media." *Applied energy* 193 (2017): 84-95.

[21]. Xu, Huijin J., Zhanbin B. Xing, F. Q. Wang, and Z. M. Cheng. "Review on heat conduction, heat convection, thermal radiation and phase change heat transfer of nanofluids in porous media: Fundamentals and applications." *Chemical Engineering Science* 195 (2019): 462-483.

[22]. Al-Abidi, Abduljalil A., Sohif Bin Mat, K. Sopian, M. Y. Sulaiman, and Abdulrahman Th Mohammed. "CFD applications for latent heat thermal energy storage: a review." *Renewable and sustainable energy reviews* 20 (2013): 353-363.

[23]. Boomsma, K., and D. Poulikakos. "On the effective thermal conductivity of a three-dimensionally structured fluid-saturated metal foam." *International Journal of Heat and Mass Transfer* 44, no. 4 (2001): 827-836.

[24]. Naterer, G. F., Advanced Heat Transfer, 3rd Edition, CRC Press, Boca Raton, FL, 2022.

[25]. Liu, Zhenyu, Yuanpeng Yao, and Huiying Wu. "Numerical modeling for solid–liquid phase change phenomena in porous media: Shell-and-tube type latent heat thermal energy storage." *Applied energy* 112 (2013): 1222-1232.

[26]. Ho, C. J., W. K. Liu, Y. S. Chang, and C. C. Lin. "Natural convection heat transfer of alumina-water nanofluid in vertical square enclosures: an experimental study." *International Journal of Thermal Sciences* 49, no. 8 (2010): 1345-1353.

[27]. Kamkari, Babak, Hossein Shokouhmand, and Frank Bruno. "Experimental investigation of the effect of inclination angle on convection-driven melting of phase change material in a rectangular enclosure." *International Journal of Heat and Mass Transfer* 72 (2014): 186-200.